

Diurnal cycle of cloud system migration over Sumatera Island

by

NAMIKO SAKURAI¹, FUMIE MURATA², MANABU D. YAMANAKA^{1,3},
SHUICHI MORI³, HAMADA JUN-ICHI³, HIROYUKI HASHIGUCHI⁴,
YUDI IMAN TAUHID⁵, TIEN SRIBIMAWATI⁵, and BUDI SUHARDI⁶

¹*Graduate School of Science and Technology, Kobe University, Kobe, Japan*

²*Disaster Prevention Research Institute, Kyoto University, Uji, Japan*

³*Frontier Observational Research System for Global Change,
Japan Marine Science and Technology Center, Yokohama, Japan*

⁴*Radio Science Center for Space and Atmosphere, Kyoto University, Uji, Japan*

⁵*Agency for the Assessment and Application of Technology (BPPT),
Jakarta Pusat, Indonesia*

⁶*Indonesian Meteorological and Geophysical Agency (BMG),
Jakarta Pusat, Indonesia*

Submitted to *J. Meteor. Soc. Japan*

8 March 2004

Abstract

This paper introduces a diurnal cycle of systematic migrations of cloud systems observed with GMS IR1 data over the whole of Sumatera Island ($\sim 1,500$ km in length) in Indonesia from May 2001 to April 2002. Convective clouds start getting active in the mountainous area in the afternoon, and migrate westward and/or eastward (~ 400 km) from midnight to morning. The westward migration appears almost every month except for the southmost part in August and December, whereas the eastward migration tends to occur mainly in/near ITCZ, which is shifted northward and southward with an annual cycle. It is considered that the westward migration may be explained by the local circulation theories, and that the eastward migration may be governed by lower-tropospheric westerly flow and/or eastward moving super clusters along ITCZ.

1 Introduction

The convective activity in the tropical area plays an important role on the global transport of water vapor and energy, hence on the global climate. They are especially active in the Indonesian maritime continent (Ramage, 1968) which consists of many islands with various sizes and is surrounded by sea water with the hottest temperature in the world. There are hierarchies of convective activities with various temporal and spatial scales from local circulation to large scale disturbance in the tropical oceans near the Indonesian maritime continent (Nakazawa, 1988).

The diurnal variation is dominant over the land in the tropics (Hendon and Woodberry, 1993). Houze et al. (1981) showed that morning precipitation over the sea near north-west Borneo (Kalimantan) Island was caused by convergence of the land breeze and monsoon wind (Johnson and Kriete, 1982). Murakami (1983) showed a contrast of diurnal cycle amplitude of deep convective activity between the land and the sea using data of the Geostationary Meteorological Satellite (GMS) black body temperature corresponding to the cloud top temperature. Nitta and Sekine (1994) confirmed this, and indicated that the convection attained its maximum intensity in late afternoon (around 19 LST) over continents and large islands, whereas in the morning (around 03 LST) over the sea in the vicinity of them. They suggested that diurnal cycles over the continents and large islands were due to strong surface heating during the daytime, and that those over the sea areas were produced by interaction between sea-land breeze circulations and large-scale environment flows. They also showed that the features of diurnal variations were different between dry and rainy seasons.

Hashiguchi et al. (1995, 1996) installed a UHF-band wind profiler (boundary layer radar) at Serpong, West Jawa, and showed clear diurnal variations of mixed layer (up to 5 km in

early afternoon) and wind (sea-land breeze circulation) in particular in the dry season. Oh-sawa et al. (2001) used data of surface rainfall and GMS with higher temporal-spatial resolutions, and pointed out that diurnal variations (especially late night-early morning maximum) of convective activities and precipitation in the Indo-China Peninsula were characterized by local circulations caused by geographical conditions. They also analyzed diurnal variations in the north-western part of Indonesia, but they did not cover the southern hemisphere side beyond the equator. Using a two-dimensional, non-hydrostatic and cloud-resolving numerical model, Satomura (2000) showed that squall lines with solar-synchronized life cycles and their eastward migrations caused the nighttime maximum of precipitation over the inland area of the Indo-China Peninsula, and that the squall lines were caused by mountain waves and cold air flows from the western part of mountains.

For the other regions, Asai et al. (1998) found that cloud systems of the east part of Tibetan Plateau migrated eastward with diurnal cycle, and suggested that wind field at 500 hPa was related to this phenomenon. In north America, Wallace (1975) found from precipitation data that the most frequent precipitation area moves eastward from the lee of the Rockies during late-night in the warm season. Riley et al. (1987) confirmed a similar migration of precipitation maximum with higher resolution data, and Meisner and Arkin (1987) reported an eastward phase shift of the diurnal cycle found from three-hourly infrared satellite data near the eastern boundary of the Rocky Mountains. Carbone et al. (2002) speculated that wave like systems in the free troposphere and/or the planetary boundary layer might contribute to the diurnal cycle of eastward migration. In the western slope of the Colombian Andes with a width of about 100 km in northwestern South America, Mapes et al. (2002a, b) and Warner et al. (2002) did both observational and numerical studies on a similar diurnal migration of clouds, and suggested that the cause of the cloud migration was a gravity wave excited by a thermal elevation over the terrain in the afternoon.

Though it is clear that the diurnal cycle is predominant in the tropics, it has not yet been understood. In particular the diurnal cycle in Sumatera Island has not been so much described. Sumatera Island is located at the west end of the Indonesian maritime continent, and covers 6°S – 6°N (the northwest-southeast extension is about 1,500 km). There are mountain districts with 2,000–3,800 m volcanos in the western part and plains spread in the eastern part (Figure 1), and the mountains play a role of barrier for flows and clouds coming from the Indian Ocean. Sakagami et al. (1990) described that rainfall amount in the western side of the mountain districts of Sumatera Island was larger than in the eastern side, and suggested that this difference might be induced by moisture which came from the Indian Ocean and was trapped on the western slope. Nitta et al. (1992) revealed that super cloud clusters propagating eastward along the equator with an intraseasonal variation received transformations over Sumatera Island, which was a particular importance of Sumatera Island among many islands in the Indonesian region.

Since 1998 many observations have been carried out by cooperations of Agency for Assessment and Application of Technology (BPPT), Meteorological and Geophysical Agency (BMG) and Institute of Aeronautics and Space (LAPAN) in the Indonesian side, and Kyoto University, Kobe University and Frontier Observational Research System for Global Change (FORSGC) in the Japanese side. Hamada et al. (2002) analyzed geographical differences of precipitation in Indonesia based on operational rain gauge data, and Hamada (2003) showed a dominant diurnal cycle of rainfall with maxima around 15–21 LST in rainy season at Bukittinggi located in the center of the mountain districts. Renggono et al. (2001) used a boundary layer radar installed at Kototabang near Bukittinggi, and showed diurnal variations of convective and stratiform rainfalls. Murata et al. (2002) showed that the diurnal variation of rainfall at Kototabang was restrained when lower tropospheric westerly wind was strong, and concluded that most of precipitation at Kototabang were not caused by large

scale disturbances but by convergence of local circulations. Wu et al. (2003) installed a GPS receiving system for precipitable water at Kototabang, and showed that water vapor was transported up to an altitude of approximately 3 km by turbulent mixing with development of the boundary layer in the afternoon and might be transported also horizontally by local circulation in dry season. Mori et al. (2004) carried out intensive rawinsonde observations at Taping in the west coast, Kototabang, and Jambi in the eastern plain area (Figure 1) several times in 2001 and 2002, and analyzed their own data together with Precipitation Radar (PR) data obtained by Tropical Rainfall Measuring Mission (TRMM) satellite, and showed that a rainfall peak in the daytime and that in the nighttime migrated from the southwestern coastline of Sumatera Island to the inland and offshore regions, respectively. They suggested that the westward migration was due to generation of new convection in windward side probably through the combination process of self-replication and gravity wave mechanisms.

The purpose of this paper is to describe detailed climatological features of the diurnal cycle of cloud system migrations, as suggested by Mori et al. (2004), over the whole of Sumatera Island throughout a year, mainly using the GMS data which are continuous in space and time rather than TRMM. The phenomenon is that cloud systems develop in the afternoon along the mountain range of Sumatera Island and migrate toward the both (west and east) coastlines for several hundreds kilometers during night. In particular we analyze *seasonal variations* of the diurnal cycle before approaching the mechanism. In Section 2, we describe data and observations. In Section 3 observational results in November 2001 are described in detail. In Section 4 statistical analysis for one year from May 2001 to April 2002 is shown. In Section 5 some discussions are made from viewpoints of diurnal variations which have been understood theoretically. Section 6 is the conclusions of this paper.

2 Observation and data description

2.1 Satellite data

A foregoing paper of our group (Mori et al., 2004) has used precipitation data observed with TRMM. Because TRMM was on a quasi-polar orbit, we could not obtain continuous temporal variations at each local position. In this paper we analyze cloud top temperature obtained with GMS, which is geostationary, so that we can analyze local temporal variations (such as traces, day-to-day variations and seasonal differences of cloud system migrations).

2.1.1 Discrimination of deep convective cloud

We used the data of black body temperature (T_{BB}) at $0.1^\circ \times 0.1^\circ$ grid points by GMS IR1 for one year (May 2001–April 2002) for analysis of the cloud top temperature. The temporal resolution is an hour. In order to discriminate deep convective clouds and omit ground temperature, a threshold value of T_{BB} must be specified.

It is known that the phase of the diurnal variation of convective activity dramatically changes with the threshold value used in the analysis (Chen and Houze, 1997). In general, the diurnal variation of convective activity evaluated by a colder threshold temperature exhibits its maximum at earlier time in the day (e.g., Minnis and Harrison, 1984; Janowiak et al., 1994). Several threshold values have been utilized in forgoing studies, and it has been pointed out that the phase of convective activity often does not correspond to that of the rainfall. Nitta and Sekine (1994) showed that the peak time of convective activity in case of

a threshold value 250 K was about 2 hours later than that of the precipitation. Thus, when discussing the diurnal variation of convective activity and rainfall together, it is desirable that the index of convective activity is defined so that their diurnal variations have the same phase. Ohsawa et al. (2001) used not only T_{BB} by the IR1 channel but also T_{BB} by the water vapor (WV) channel and showed that the difference $T_{\text{BB}} \equiv T_{\text{BB}}(\text{IR1}) - T_{\text{BB}}(\text{WV}) < 3$ K had good correlation with an intensive rainfall and also corresponded to a cloud-top temperature $T_{\text{BB}} < 230$ K. Therefore, as some forgoing studies (e.g., Hendon and Woodbery, 1993; Satomura, 2000), the threshold value (T_c) 230 K is adopted in this study and T_{BB} index ($I_{T_{\text{BB}}}$) is defined as follows:

$$I_{T_{\text{BB}}} = \begin{cases} T_c - T_{\text{BB}} & \text{for } T_{\text{BB}} \leq T_c \\ 0 & \text{for } T_{\text{BB}} > T_c. \end{cases}, \quad (1)$$

In the present case 230 K corresponds to the air temperature at an altitude around 11 km, and $I_{T_{\text{BB}}}$ is used to omit clouds lower than 11 km.

Furthermore, in this study an occurrence frequency α of $I_{T_{\text{BB}}}$ ($T_{\text{BB}} \leq 230$ K) at each pixel and time is calculated for a month, as follows:

$$\alpha \equiv \frac{(\text{The number of } I_{T_{\text{BB}}} > 0)}{(\text{The total number of valid data for a month})} \times 100, \quad (2)$$

which indicates how frequently convective clouds penetrate above the 11 km altitude. We did not calculate a monthly value of α , if the number of lack of data exceeds 4 for one month.

(1) and (2) are also used to define inter-tropical convergence zone (ITCZ) at 100°E. We

used 270 K for 230 K into T_c because we define areas where cloud coverage is high ITCZ since in ITCZ convection is always active, and analysis period is changed one month to 5 days. We defined areas where α is more than 50 % ITCZ at 100°E.

2.1.2 Cross-section analysis over Sumatera Island

Sumatera Island has mountain districts in the western part and plains in the eastern part (see Figure 1). Local winds reversed with a diurnal cycle due to sea-land or mountain-valley breeze circulations may exist and they are considered to be perpendicular to the coastlines or mountain ridge. Therefore five cross-sections (AA', BB', CC', DD', and EE' in Figure 1) which are approximately perpendicular to the coastlines and mountain ridge of Sumatera Island are analyzed. The phase of seasonal variation in each cross-section may be inhomogeneous (cf. Hamada et al., 2003), since Sumatera Island is extended over the both hemispheres beyond the equator.

2.2 Rawinsonde data

In Indonesia, BMG launches rawinsondes operationally at eleven stations but not every day (Okamoto et al., 2003). Tabing (100.35°E, 0.88°S, 3 m MSL) is one of those operational stations and rawinsondes have been launched at 0000 UTC (0700 LST) every other day usually.

Several Indonesian and Japanese institutions (see Section 1; also Mori et al., 2004) have been carried out intense rawinsonde observations for seven periods (May–June, August, and November 2001; April and November 2002; July and November 2003) at three stations: Tabing, Kototabang (100.32°E, 0.20°S, 865 m MSL), and Jambi (103.64°E, 1.63°S, 26 m

MSL) in Sumatera Island (see Figure 1). The duration of each intense observation period (IOP) is 4 weeks. Tabing, Kototabang, and Jambi are located near the western coast, in the mountain districts, and in the plains around 100 km inland from the eastern coast, respectively. The former two stations are roughly located along the cross-section CC' in Figure 1, and the last station is on DD'. We employed the receiver and transmitters of a GPS-rawinsonde system (Vaisala RS-15GH) with meteorological balloons (TOTEX TA-1000 type for daytime, and TX-1000 type for night-time) at Kototabang and Jambi, and a radar tracking rawinsonde system (Meisei RS3-89A transmitters and a Weather Tronics receiver) at Tabing. The both rawinsonde systems can get vertical profiles of temperature, relative humidity, pressure, and zonal and meridional winds with a vertical resolution of 100 m.

In this study we analyzed mainly the data observed in November 2001. This period corresponds to one of two rainy seasons during March–May, and September–November in the central part of Sumatera (Hamada et al., 2002), which appear due to the annual variation (north–south shift around the equator) of ITCZ (Murakami and Matsumoto, 1994; Okamoto et al., 2003). Rawinsondes have been launched 4 times per day at around 0030, 0630, 1230, and 1830 LST (corresponding to observations for analysis at 1800, 0000, 0600 and 1200 UTC) in the first and fourth weeks, and 8 times per day at 0030, 0330, 0630, 0930, 1230, 1530, 1830 and 2130 LST (for analysis at 1800, 2100, 0000, 0300, 0600, 0900, 1200 and 1500 UTC) in the second and third weeks at Kototabang and Jambi stations in November 2001.

2.3 Equatorial atmosphere radar (EAR)

A VHF (47.0 MHz) Doppler radar with an active phased-array antenna system (a peak output power of 100 kW, approximately 110 m in diameter, and 560 three-element Yagi antennas), called the Equatorial Atmosphere Radar (EAR) has been operated at Kotota-

bang since June 2001 (Fukao et al., 2003). It detects three-dimensional atmospheric motion (including vertical component) in an altitude range of 2–20 km on both clear and rainy conditions, and does also precipitation particle motion on rainy condition. The time resolution is about 90 s, the vertical resolution is about 150 m. By using the high time resolution of EAR, which is far higher than rawinsondes even in the intense observational periods, we can obtain detailed time evolution features of the diurnal cycle. In this paper EAR data in November 2001 is used for the analysis.

2.4 Objective analysis data

Objective analysis data (NCEP/NCAR) provided by the US National Weather Service are used. The spatial resolution and analysis period are $2.5^{\circ} \times 2.5^{\circ}$ grid points and one year (May 2001–April 2002), respectively. The temporal resolution is 6 hours (0000, 0600, 1200, and 1800 UTC). The vertical resolution is 17 standard pressure levels from 1,000 to 10 hPa.

3 Diurnal cycle observed in November 2001

3.1 Migrations of cloud system

Figure 2 shows horizontal distributions of the occurrence frequency α of tall cloud systems in November 2001. Convection gets active in the mountain districts of Sumatera Island and their western side in the afternoon (15 LST). In the evening (18 LST) tall cloud systems are concentrated in the western part of Sumatera Island. In the night (21, 00 and 03 LST) the cloud systems are separated and migrate both westward and eastward. In the morning (06 and 09 LST) they are over the seas off the both coastlines of Sumatera Island. It is found that such diurnal cycle of the cloud system migration occurs systematically over the whole of Sumatera Island.

Figure 3 is time-longitude cross-sections of α along the five lines defined in Subsection 2.1.2 and Figure 1. Convective activities are the most active along DD'. α gets up to peak in the evening in the mountainous area at around 17 LST, except for DD' at around 20 LST. Westward migration starts just after getting up to peak (17 LST), and eastward migration is from around 23 LST along AA', BB' and CC'. Along DD' and EE' migrations start both westward and eastward almost simultaneously after getting up to peak (20 LST in DD' and 17 LST in EE'). Table 1 shows migratory velocities and distances of cloud systems along each cross-section, calculated by tracing: peaks of α from starting at the mountainous area until stopping or disappearance and by using method of least squares. Along AA' and BB' values of the migratory velocities and distances in case of westward migration are larger than those of eastward migration, whereas along CC', DD', and EE' westward migration is smaller than eastward one. We find that the order of eastward migratory velocities and distances (DD', CC', EE', BB', and AA') depends on width of the land.

Figure 4 shows time-longitude cross-section of T_{BB} with GMS IR1 data in November

2001 on the equator. In this period three super cloud clusters with a time scale longer than a few days pass over Sumatera Island. One super cloud cluster moves eastward, and cloud clusters shorter than a few days migrate westward during November 3–10. During November 11–18 and 22–30 the other two super cloud clusters including cloud clusters pass eastward over Sumatera Island. The clusters with the shorter time scales move eastward in the east of 100°E over Sumatera Island on November 4–7, 12, 13, 19, 22, 25 and 29.

3.2 Wind variations

In this subsection we present wind variations during the same period as described in the previous subsection from larger to smaller scales. Figure 5 shows vertical-zonal cross-section of horizontal wind and relative humidity averaged for 12 UTC (19 LST) through November 2001 on the equator. Because November is in rainy season over central (equatorial) Sumatera (not all over Indonesia; see Hamada et al., 2003), relative humidity is especially high throughout the troposphere over the corresponding longitudinal region. The fact that humidity is especially high over the land is consistent with the diurnal cycle features of cloud systems shown in Figure 2. On the equator westerly wind blows below 600 hPa, and easterly one does above 500 hPa.

Figure 6 shows mean diurnal variations of zonal wind observed with EAR and rawinsondes during November 1–28 at Kototabang. The EAR data are averaged every 1 hour before taking 28-day mean. Both results are almost the same, in spite that time resolution of rawinsonde data (6 hours) is much lower than that of EAR one (1 hour): westerly (easterly) wind blows below (above) 7 km, and westerly wind at around 13 LST (19 LST) is weak (strong). Thus we consider that rawinsonde data can express characteristics of diurnal variation of zonal wind sufficiently at least for our purpose in this study.

The background wind structure with westerly (easterly) below (above) 6–7 km through-

out a day was also confirmed by rawinsondes launched at Jambi during November 1–28, as shown in mean vertical profiles of Figure 7.

Panels of Figure 7 show zonal wind anomalies (from the mean wind profiles in each right-hand side) at the two stations averaged for days in which the eastward or westward migrations of cloud systems. In case of westward migration of cloud systems, zonal wind anomaly at Kototabang in 1.5–5.5 km is anti-phase to that in 10–12 km for which the temperature is close to the threshold value 230 K of GMS clouds shown in Figure 2, but such anti-phase features are not clear at Jambi. In case of eastward migration, somewhat shifted (about 1/4 cycle or 6 hours delayed) anti-phased structures between lower (1.5–5.5 km) and upper (10–12 km) layers are found at both stations.

4 Statistical analysis during May 2001–April 2002

4.1 Seasonal variation of migratory directions of cloud systems

Migratory directions of cloud systems during May 2001–April 2002 are determined, based on the cross-section analysis as shown in Figures 3 and 8. Occurrence of westward and/or eastward migrations are defined as follows: peaks of α larger than 10 % start migrating from the mountainous area during 12–24 LST and arrive at each coast until next morning. The total results are shown in Table 2. Blanks represent that α is less than 10 % or migration of cloud systems is not observed clearly in such monthly analysis, probably because convective activities are weak or diurnal cycle is not so dominant.

Figure 8 shows time-latitude cross-sections of α along CC' (roughly in the center of Sumatera Island) during May 2001–April 2002. In May and June both westward and eastward migrations occur, and α for both directions decrease in June. In July we find only westward migration and α is small. In August we have both directions again. Westward migration is dominant in September and α is larger than in August. In October, November and December we have both westward and eastward migrations and α takes maxima in November. In January, February and March westward migration occurs and α increases. In March cloud systems which migrate eastward do not reach the east coast, though eastward migration occurs. In April we have migrations of both directions.

Figure 9 shows time-longitude cross-section of horizontal wind at 850 hPa along the equator (near CC') around Sumatera Island. During October–December westerly wind is stronger than in other seasons over Sumatera Island. Eastward migration of cloud systems appears more frequently in this period than the other seasons (see Figure 8). On the other hand, easterly wind blows in September and January over Sumatera Island, and eastward migration of cloud systems does not appear at all and only westward migration is observed

(see Figure 8).

Table 2 shows that the westward migration appears in almost all the cross-sections and seasons, except for EE' in August and December. Along EE' a cloud which grows up to levels with temperature lower than 230 K is hardly observed in July and August. On the other hand, the eastward migration has a tendency of seasonal variation. The north-south width of the areas where the eastward migration appears is narrower than that of Sumatera Island, and looks like shifting northward from May to July. It extends southward from August to December, and stays in the southern part of Sumatera Island during January–February. It extends northward from March. Therefore, the area of the eastward migration tends to oscillate around the equator with an annual cycle and to shift toward summer hemisphere around a solstice season. For CC' and DD' along which the distance between mountain range and eastern coast line is wider than in the other cross-sections, cloud systems do not arrive at the eastern coast, though they migrate eastward from mountainous area in March and April 2002. Including such cases (marked with \square in Table 2), the annual north-south shift of eastward migratory area is shown clearly.

4.2 Comparison with large scale features

ITCZ also oscillates northward and southward with an annual cycle around the Indonesian maritime continent region (see, e.g., Murakami and Matsumoto, 1994; Okamoto et al., 2003). Although ITCZ is sometimes not so clear over the Indonesian maritime continent, we defined the location of ITCZ at 100°E during May 2001 to April 2002 (see Subsection 2.1.1) as shown in Figure 10(a).

During May–July ITCZ shifts northward. In July the center of ITCZ is located around 20°N (northern Thailand). In mid-July the summer monsoon over Southeast Asia is at its

peak. After July ITCZ begins to shift southward. In November, the whole of Sumatera Island is covered with ITCZ, and just in this month α is especially high. Then ITCZ continues to go southward, arriving at around 10°S in January and February. From March to April, ITCZ goes northward again, and the center of ITCZ passes the equator. These annual-cycle features of ITCZ are quite similar to the oscillatory movement of the area where cloud systems migrate eastward shown in Table 2.

Figures 10(b) and (c) show time-latitude cross-sections of horizontal wind at 100°E in the upper and lower troposphere over Sumatera Island, respectively. During May–August westerly at 850 hPa takes maximum around 10°N where cloud amount associated with ITCZ is also large. This zonal wind structure shifts southward from September to December, and westerly wind at 850 hPa almost disappears during late December–January when the cloud amount takes a minimum. From February the wind structure associated with ITCZ returns northward. On the other hand, in the upper troposphere easterly wind area covers ITCZ and Sumatera Island almost throughout the analysis period.

The movement of ITCZ and zonal wind structure for the period analyzed here is similar to the climatological feature of ITCZ investigated using OLR data derived from NOAA for different period by Murakami and Matsumoto (1994) and operational rawinsonde data by Okamoto et al. (2003). Thus ITCZ in the observational period is not abnormal, and we consider that similar features of the diurnal cycle of cloud activities reported in this paper must appear every year.

5 Discussions

5.1 Relationship between water vapor, cloud and rainfall

This paper mainly concerns features of cloud systems. In this subsection we shall compare our results with earlier results on features of water vapor and rainfall obtained by our group, although the latter is still limited in space and time.

5.1.1 Water vapor supply for cloud development

In the western slope of Sumatera Island it is considered that sufficient water vapor generating clouds may be supplied from the Indian Ocean, because the distance between the west coastline and the mountain ridge is short (~ 50 km). As mentioned in Section 1, Wu et al. (2003) have described evidence of diurnal variations of column density of water vapor at Kototabang observed by GPS radio-wave analysis as well as rawinsondes. They speculate that water vapor may be transported both vertically (from the ground surface through turbulent mixing in the boundary layer) and horizontally (from Indian ocean through westerly wind) in the afternoon. They concern observations only at one station and during a limited period in dry season (August 2001), but we consider that similar processes may work also in other seasons in other areas in the western part of Sumatera Island.

Although westerly in the lower troposphere is dominant almost throughout a year (except for short periods around September and January) almost all over Sumatera (see arrows near 100°E in Figure 9), and particularly in/around November (as shown also in Figures 5-7), such background flow cannot explain diurnal variations. Furthermore, as Murata et al. (2002) have shown, too strong westerly probably due to intraseasonal variations seems to suppress generation of cloud and precipitation at Kototabang. However, the westerly

anomaly observed near the surface at Kototabang (see Figure 7) in the afternoon seems consistent with such water vapor supply for cloud generation near the mountain range in the early evening. As will be discussed in Subsection 5.2.1, this westerly anomaly is consistent with a sea breeze, and is considered to be withdrawn to the west coastline until the morning.

In the eastern slope of Sumatera Island, the distance between the east coastline and the mountain ridge may be too far (~ 300 km) to receive water vapor by a sea breeze from the strait of Malacca. The lower-tropospheric background wind which is westerly (eastward) almost throughout a year as mentioned above is not appropriate for water vapor transport toward mountainous areas (westward) from the eastern coast, and water vapor transported from Indian Ocean by the background westerly is considered to be consumed for precipitation in the western slope of the mountain ridge ($\sim 3,000$ m) (cf. Sakagami et al., 1990; Hamada, 2003). Therefore, we must consider much more special conditions to generate deep convective cloud in the eastern part of Sumatera. Actually, eastward migration appears in/near ITCZ with seasonal variation (see Subsection 4.2), and ITCZ is indeed a convergence zone of water vapor flux. Such a contribution of large-scale processes will be discussed again in Subsection 5.2.2.

5.1.2 Convective cloud system and rainfall

In foregoing studies of our group, Renggono et al. (2001) have studied diurnal and seasonal variations of rainfall at Kototabang (and also at a station near Jakarta, West Jawa), based on profiler radar echo analysis, and have shown a peak of convective rainfall occurrence at around 14 LST and that of stratiform rainfall peak at around 18 LST. From automatic raingauge measurement (cf. Hamada, 2003) for four years (1999–2002) at Kototabang, the diurnal rainfall peaks occurred during 15–17 LST in both of two rainy seasons (March–May

and September–November) and at around 18 LST in two dry (or minimum rainfall) seasons (around June and around January). Combining these features with the results in this paper, we find that the tall cloud systems generated during 15–18 LST in the mountainous areas (see Figure 2) provide the afternoon-evening rainfall peaks observed at Kototabang, which are due to tall convective clouds in an earlier stage (around 15 LST) and due to stratiform clouds below high anvils in a later stage (around 18 LST).

Mori et al. (2004) have done more systematic analysis on the diurnal rainfall cycle using the TRMM space-borne radar. The radar covers the whole of Sumatera Island, but their detailed analysis is mainly only for the central part of Sumatera including Kototabang. Their results on rainfall peak migrations (Figure 5 of their paper) are roughly consistent with our results on the tall cloud system migrations (a cross-section panel along CC' in Figure 3 and panels in Figure 8). They have distinguished convective and stratiform rainfalls which are also consistent with the results at Kototabang by Rengonno et al. (2001) mentioned above. Some differences between their and our results, such as a separation between evening mountainous-area convective rainfall (15–24 LST, seemingly associated with eastward migrations) and morning coastal half-stratiform rainfall (22–09 LST, associated with westward migrations), are found, but their results on rainfall peaks from integration of discontinuous data for three years are not directly comparable with our results on tall clouds from continuous observations. They also show another separated (relatively weaker) rainfall peak in the eastern coast in the morning (around 04 LST). Relative humidity increase associated with temperature minimum before sunrise may be taken into account in order to consider the morning rainfall peaks in the both coastal regions, which may not necessarily be dependent upon tall cloud system activities.

Murata et al. (2002) have confirmed the afternoon-evening rainfall peaks at Kototabang during a limited observation period (September–October 1998), and have shown that they

tend to disappear when the lower tropospheric westerly is stronger than 10 ms^{-1} . This westerly increase is clearly associated with some intraseasonal variations which are also accompanied with cloud (super) clusters in the Indian Ocean. This implies that such clusters disappear just before landing Sumatera Island, as suggested so far by Nitta et al. (1992), and that rainfall in Sumatera is not directly produced by the clusters moving eastward from the Indian Ocean. In our study, such disappearance of cloud clusters just before landing Sumatera can be confirmed in Figure 4, and some cloud systems generated with the diurnal cycle in the mountainous area of Sumatera seem to move eastward, which are the eastward migration cases found in this paper. The cloud-system eastward migration (or re-starting) from Sumatera appears only inside/near ITCZ shifting north-southward with a seasonal (annual) cycle, as shown in Subsection 4.2. This may be considered as an interaction between local and large-scale phenomena, which will be discussed again in Subsection 5.2.2.

5.2 Mechanisms of cloud system migrations

The diurnal cycle of cloud systems which migrate westward and eastward over Sumatera Island has been demonstrated in Subsections 3.1 and 4.1. Directions of zonal wind anomaly at Kototabang and Jambi shown in Subsection 3.2 are consistent with convergence and divergence associated with the cloud systems which migrate westward or eastward (see Figure 11). However, the appearance tendencies of westward and eastward migrations are different. Westward migration appears in almost all seasons and areas, whereas eastward migration has seasonal variation following the north-south displacement of ITCZ (see Figure 12). Therefore, mechanisms generating westward and eastward migrations may not be common.

5.2.1 Local circulations

The westward migration does not depend on seasons. Thus some local circulations (sea-land and mountain-valley breezes) which have been known as a dominant feature in the tropics (see Section 1) may be related with the westward migration. The diurnal wind variations observed in the lowest 1 km at Kototabang (in particular for westward migration case) are easterly (from the mountain range) in the morning and westerly (from the Indian Ocean) in the evening, which are consistent with such a circulation in an inland region. Classical (linear) theories on the sea-land breeze circulation (e.g., Jeffreys, 1922; Defant, 1951; Rotunno, 1983; Niino, 1987), which are mathematically equivalent to those on inertio-gravity waves (cf. Satomura, 2000; Carbone et al., 2002; Mapes et al., 2002b; Mori et al., 2004), have shown that the horizontal and vertical scales (L and H , respectively) of such a circulation have a ratio given approximately by

$$\frac{L}{H} \sim \frac{N}{2\pi/24\text{hours}}, \quad N = \sqrt{g \frac{\partial \ln \theta}{\partial z}}, \quad (3)$$

where N is the Brunt-Väisälä frequency, g is the gravity acceleration ($= 9.8 \text{ m/s}^2$), θ is potential temperature and z is altitude. If we substitute (dry) potential temperature obtained by rawinsonde data (shown in Figure 7) into θ , then $N \sim 10^{-2} \text{ s}^{-1}$, and $L/H \sim 10^2$. Then, if the height of a local circulation cell H is $\sim 1 \text{ km}$, we have the width of the cell L must be $\sim 1.5 \times 10^2 \text{ km}$, which is comparable to three times of the distance between the west coastline and the mountain ridge in Sumatera Island. A mountain-valley circulation may strengthen the sea-land breeze circulation, because the both circulations are considered to

have similar size and phase. Therefore, a land (or mountain) breeze front associated with convective clouds may explain the westward migration from the mountainous area to the coastal area in the nighttime as considered in the classical sea-land breeze (or inertio-gravity wave) theories. Generation mechanism of new convective cloud in the migratory direction (windward side of a old cloud) must be also considered, as suggested by Mori et al. (2004), but detailed cloud-physical consideration is impossible as long as we have not yet done any sufficient observations in the intermediate area between mountainous and coastal regions.

We shall consider whether a similar consideration can be applied to the eastward migration. Local circulations may occur also in the eastern side of Sumatera Island. However, if N and H are not so different from those in the western side, L also must be similar to that in the western side (~ 150 km), which is clearly shorter than twice of the distance between the east coastline and the mountain ridge along CC' , DD' and EE' . Thus mountain-valley and sea-land breeze circulations are hardly strengthened with each other. Although the distances between the both coastlines and the mountain ridge are similar along AA' and BB' , eastward migration has seasonal change. It is supposed that other cases may be responsible for eastward migration because eastward one is not explained by classical (linear) theory on the sea-land breeze circulation.

5.2.2 Effects of large-scale phenomena

Background wind may be related with migratory direction of cloud systems, because foregoing studies (Asai et al., 1998; Satomura, 2000) pointed out the relationship with between cloud system migration and background wind, as noted also by our forgoing study (Mori et al., 2004). In the upper troposphere at 100°E , easterly wind is dominant throughout the year (Figure 10), and westward migration appears in almost all the seasons except for August and

December 2001 in the southern part of Sumatera Island (EE'). However, we cannot relate the eastward migration with the upper-tropospheric easterly, because the lower-tropospheric dominant wind is westerly as Mori et al. (2004) have mentioned, and the occurrence of eastward migration has a clear seasonal dependence. For December 2001 along EE', westerly wind blowing at all the altitudes may be related to the eastward migration observed there.

On the other hand background wind in the lower troposphere is westerly in annual-mean zonal component, which is similar to the eastward migration velocity, as suggested by Mori et al. (2004). Furthermore, it has seasonal variations. The cross-equatorial monsoon circulation is south-easterly in the southern-hemispheric side and south-westerly in the northern-hemispheric side in the northern summer season, and it is north-easterly in the northern-hemispheric side and north-westerly in the southern-hemispheric side in northern winter (Murakami and Matsumoto, 1994; Okamoto et al., 2003). This circulation converges into ITCZ which is located in northern (southern) hemisphere in northern summer (winter). Thus, westerly wind blows in ITCZ, and eastward movement of super cloud clusters appears frequently (Nakazawa, 1988). Such a super cluster has an intraseasonal temporal scale and involves smaller-scale clusters which move mainly westward over the Pacific, but does not have clear zonal propagation over Sumatera. In November 2001 around the equator eastward migration tends to appear when super cloud clusters propagate eastward from the Indian Ocean and pass over Sumatera Island (Figure 4). Thus it is considered that the lower-tropospheric background westerly and cloud disturbances in ITCZ are related to the eastward cloud migration.

6 Conclusions

In this paper we have described a systematic cloud migration with diurnal cycle over Sumatera Island (northwest-southeast length $\sim 1,500$ km), based on GMS IR1 data and intense observations with rawinsondes and a wind profiler. Cloud systems start growing up to 11 km in the mountainous area in the western part of Sumatera Island in the afternoon, and migrate for a distance of several hundreds kilometers both westward and eastward from night to morning.

By a climatological analysis for one year (May 2001–April 2002), the westward migration with diurnal cycle appears in almost all the seasons and almost all over the western part of Sumatera, except for August and December in the southern end, whereas the eastward migration with diurnal cycle is observed only in a zone which is shifted northward and southward with an annual cycle. The zone where the eastward migration appears is identified with ITCZ approximately.

The westward migration may be explained by the classical sea-land breeze theories, but these theories may not be applied to the eastward migration, because the distance between the east coastline and the mountain range is too long, and the appearance has clear seasonal and meridional variations as mentioned above. For the eastward migration we consider that it is related to features in ITCZ; westerly wind in the lower troposphere is dominant and super cloud clusters are moving eastward in ITCZ around 100°E .

The existence of the diurnal cycle of systematic cloud generation and migration over the whole island of Sumatera must be quite important to consider behaviors of super clusters or intraseasonal variations passing this region, as so for suggested by Nitta et al. (1992) and Nitta and Sekine (1994). Such phenomena with horizontal scales of more than 1,000 km and temporal scales of one day or shorter are not so easy to be simulated by usual general

circulation models, nor to be understood by dynamical theories so far presented. We are going to continue intense observations in Sumatera, under collaborations with instruments used in Murata et al. (2002), Wu et al. (2003) and Mori et al. (2004).

Acknowledgments

We heartly thank colleagues of BPPT, BMG, and LAPAN in the Indonesian side, and Kyoto University, Kobe University, and FORSGC in the Japanese side for their strong collaborations in observations. We thank Prof. T. Yasunari of Nagoya University, Prof. T. Satomura of Kyoto University, and Prof. S. Fukao and Dr. N. Kawano of RASC, Kyoto University for their useful suggestions, comments and encouragement. The EAR belongs to RASC of Kyoto Universty, Japan and is operated by RASC and LAPAN, Indonesian based upon the agreement between RASC and LAPAN signed on September 8, 2000.

References

- Asai, T., S. Ke, and Y. Kodama, 1998: Diurnal variability of cloudiness over east asia and the Western Pacific Ocean as revealed by GMS during the warm season, *J. Meteor. Soc. Japan*, **76**, 675-684.
- Carbone, R.E., J.D. Tuttle, D.A. Arijevych, and S.B. Trier, 2002: Inferences of predictability associated with warm precipitation episodes, *J. Atmos. Sci.*, **59**, 2033-2056.
- Chen, S. and R.A. Houze, 1997: Diurnal variation and life-cycle of deep convective systems over the tropical Pacific warm pool, *Quart. J. Roy. Meteor. Soc.*, **123**, 357-388.
- Defant, F., 1951: Local winds, *Compendium of Meteorology*, American Meteorological Society, 655-672.
- Fukao, S., H. Hashiguchi, M. Yamamoto, T. Tsuda, T. Nakamura, M.K. Yamamoto, T. Sato, M. Hagio, and Y. Yabugaki, 2003: Equatorial atmosphere radar (EAR): System description and first results, *Radio Sci.*, **38**, 3, 1053, doi:10.1029/2002RS002767.
- Hamada, J.-I., 2003: A climatological study on rainfall variations over the Indonesian maritime continent, Doctoral thesis, Graduate School of Science, Kyoto University.
- Hamada, J.-I., M.D. Yamanaka, J. Matsumoto, S. Fukao, P.A. Winarso, and T. Sribimawati, 2002: Spatial and temporal variations of the rainy season over Indonesia and their link to Enso, *J. Meteor. Soc. Japan*, **80**, 285-310.
- Harada, J., T. Oki and K. Murakami, 1998: Diurnal variation and its seasonal variation of convective activity over the Indochina Peninsula region by GMS-IR data, *J. Soc. Hydrol. Water Resour.*, **11**, 371-381. (in Japanese with abstract in English)

- Hashiguchi, H., S. Fukao, T. Tsuda, M.D. Yamanaka, D.L. Tobing, T. Sribimawati, S.W.B. Harijono, and H. Wirjosumarto, 1995: Boundary layer radar observations of the passage of the convection center over Serpong, Indonesia during the TOGA COARE intensive observation period, *J. Meteor. Soc. Japan*, **73**, 535-548.
- Hashiguchi, H., S. Fukao, M.D. Yamanaka, S.W.B. Harijono and H. Wirjosumarto, 1996: An overview of the planetary boundary layer observations over equatorial Indonesia with an *L*-band clear-air Doppler radar, *Beitr. Phys. Atmosph.*, **69**, 13-25.
- Hendon, H.H. and K. Woodberry, 1993: The diurnal cycle of tropical convection, *J. Geophys. Res.*, **98**, 16623-16637.
- Houze, R.A., S.G. Geotis, J.F.D. Marques, and A.K. West, 1981: Winter monsoon convection in the vicinity of north Borneo. Part I: Structure and time variation of the clouds and precipitation, *Mon. Wea. Rev.*, **109**, 1595-1614.
- Janowiak, J.E., P.A. Arkin, and M. Morrissey, 1994: An examination of the diurnal cycle in oceanic tropical rainfall using satellite and in situ data, *Mon. Wea. Rev.*, **122**, 2296-2311.
- Jeffreys, H., 1922: On the dynamics of wind, *Quart. J. Roy. Meteor. Soc.*, **48**, 29-46.
- Johnson, R.H. and D.C. Kriete, 1982: Thermodynamic and circulation characteristics of winter monsoon tropical mesoscale convection, *Mon. Wea. Rev.*, **110**, 1898-1911.
- Mapes, B.E., T.T. Warner, M. Xu and A.J. Negri, 2002: Diurnal patterns of rainfall in northwestern South America. Part I: Observations and context, *Mon. Wea. Rev.*, **131**, 799-812.
- Mapes, B.E., and M. Xu, 2002: Diurnal patterns of rainfall in northwestern South America.

- Part III: Diurnal gravity waves and nocturnal convection offshore, *Mon. Wea. Rev.*, **131**, 830-844.
- Meisner, B.N., and P.A. Arkin, 1987: Spatial and annual variations in the diurnal cycle of large-scale tropical convective cloudiness and precipitation, *Mon. Wea. Rev.*, **115**, 2009-2032.
- Minnis, P. and E.F. Harrison, 1984: Diurnal variability of regional cloud and clear-sky radiative parameters derived from GOES Data. PartII: November 1978 cloud distributions, *J. Appl. Meteor.*, **23**, 1012-1031.
- Mori, S., Hamada, J.-I., Y.I. Tauhid, M.D. Yamanaka, N. Okamoto, F. Murata, N. Sakurai, and T. Sribimawati, 2004: Diurnal land-sea rainfall peak migration over Sumatera Island, Indonesian maritime continent observed by TRMM satellite and intensive rawinsonde soundings, *Mon. Wea. Rev.*, **132**, in press.
- Murakami, M., 1983: Analysis of the deep convective activity over the western Pacific and Southeast Asia. Part I, *J. Meteor. Soc. Japan*, **61**, 60-76.
- Murakami, T. and J. Matsumoto, 1994: Summer Monsoon over the Asian Continent and Western North Pacific, *J. Meteor. Soc. Japan*, **72**, 719-745.
- Murata, F., M.D. Yamanaka, F. Fujiwara, S. Ogino, H. Hasiguchi, S. Fukao, M. Kudsy, T. Sribimawati, S.W.B. Harijono and E. Kelana, 2002: Relationship between wind and precipitation observed with a UHF radar, GPS rawinsondes and surface meteorological instruments at Kototabang, West Sumatera during September–October 1998, *J. Meteor. Soc. Japan*, **80**, 347-360.
- Nakazawa, T., 1988: Tropical super clusters within interseasonal variations over the western pacific, *J. Meteor. Soc. Japan*, **66**, 823-839.

- Niino, H., 1987: The linear theory of land and sea breeze circulation, *J. Meteor. Soc. Japan*, **65**, 901-921.
- Nitta, T., T. Mizuno and K. Takahashi, 1992: Multi-scale convective systems during the initial phase of the 1986/87 El Niño, *J. Meteor. Soc. Japan*, **70**, 447-466.
- Nitta, T. and S. Sekine, 1994: Diurnal variation of convective activity over the tropical western pacific, *J. Meteor. Soc. Japan*, **72**, 627-641.
- Ohsawa, T., H. Ueda, T. Hayashi, A. Watanabe and J. Matsumoto, 2001: Diurnal variations of convective activity and rainfall in tropical Asia, *J. Meteor. Soc. Japan*, **79**, 333-352.
- Okamoto, N., M.D. Yamanaka, S. Ogino, H. Hashiguchi, N. Nishi, T. Sribimawati, and A. Numaguti, 2003: Seasonal variations of tropospheric wind over Indonesia: Comparison between collected operational rawinsonde data and NCEP reanalysis for 1992–99, *J. Meteor. Soc. Japan*, **81**, 829-850.
- Ramage, C.S., 1968: Role of a tropical “maritime continent” in the atmospheric circulation, *Mon. Wea. Rev.*, **96**, 365-369.
- Renggono, F., H. Hashiguchi, S. Fukao, M.D. Yamanaka, S.-Y. Ogino, N. Okamoto, F. Murata, B.P. Sitorus, M. Kudsy, M. Kartasasmita and G. Ibrahim, 2001: Precipitating clouds observed by 1.3-GHz boundary layer radars in equatorial Indonesia, *Annales Geophysicae.*, **19**, 889-897.
- Richards, F. and P. Arkin, 1981: On the relationship between satellite-observed cloud cover and precipitation, *Mon. Wea. Rev.*, **109**, 1081-1093.
- Riley, G.T., M.G. Landin, and L.F. Bosart, 1987: The diurnal variability of precipitation across the central Rockies and adjacent Great Plains, *Mon. Wea. Rev.*, **115**, 1161-1172.

- Rotunno, R., 1983: On the linear theory of the land and sea breeze, *J. Atmos. Sci.*, **40**, 1999-2009.
- Sakagami, F.R. Ohgushi, and D.W. Roubik, 1990: *Natural History of Social Wasps and Bees in Equatorial Sumatra*, Hokkaido University Press, Sapporo, Japan, 274pp.
- Satomura, T., 2000: Diurnal variation of precipitation over the Indo–China Peninsula: Two-dimensional numerical simulation, *J. Meteor. Soc. Japan*, **78**, 461-475.
- Wallace, J.M., 1975: Diurnal variations in precipitation and thunderstorm frequency over the continental United States, *Mon. Wea. Rev.*, **103**, 406-419.
- Warner, T.T., B.E. Mapes and M. Xu, 2002: Diurnal patterns of rainfall in northwestern South America. Part II: Model simulations, *Mon. Wea. Rev.*, **131**, 813-829.
- Wu, P.-M., J.-I. Hamada, S. Mori, Y.I. Tauhid, M.D. Yamanaka, and F. Kimura, 2003: Diurnal variation of precipitable water over a mountainous area of Sumatra Island, *J. Appl. Meteor.*, **42**, 1107-1115.

Table and figure captions

Table 1. Migratory distance and speed of tall cloud systems (cloud top temperature ≤ 230 K) along each cross-section over Sumatera Island in November 2001.

Table 2. Seasonal-'meridional' distributions of occurrence of westward and eastward migrations (see text for definitions) of tall cloud systems (cloud top temperature ≤ 230 K) during May 2001–April 2002.

Figure 1. Topography of Sumatera Island. Tabing, Kototabang, and Jambi are stations operated for intensive observational periods in 2001 and 2002. Along five lines from AA' to EE', diurnal cycle of cloud system migration will be analyzed in subsequent figures and sections.

Figure 2. Horizontal distributions of the occurrence frequency α of tall cloud systems (cloud top temperature ≤ 230 K) at each pixel and time every 3 hour over Sumatera Island and surroundings in November 2001. Definition of α is given by (2) in the text.

Figure 3. Local time-longitude cross-sections of the occurrence frequency α of tall cloud systems (cloud top temperature ≤ 230 K) at each pixel along the five lines from AA' to EE' shown in Figure 1 during November 2001. Vertical solid and broken lines represent locations of coasts of Sumatera Island (for CC' also of Mentawai Archipelago and Malay Peninsula) and of 800 m MSL, respectively.

Figure 4. Time-longitude cross-section of T_{BB} on the equator in November 2001, based on GMS IR1 data with a spatial resolution of $0.5^\circ \times 0.5^\circ$ grid points. The vertical solid line indicates 100°E

which corresponds to the location of the central mountain range of Sumatera Island on the equator.

Figure 5. Vertical-zonal cross-section of horizontal wind (arrows; upward is northward) and relative humidity (shaded is larger than 60 %) on the equator at 12 UTC (19 LST) averaged for November 2001, based on the NCEP/NCAR objective analysis. The solid lines indicate the coasts of Sumatera Island.

Figure 6. Vertical-local time cross-sections of mean diurnal variation of zonal wind observed with (a) EAR and (b) rawinsondes at Kototabang in November 2001. Broken line in (a) represents the altitude at Kototabang (865 m).

Figure 7. Vertical-local time cross-sections of zonal wind anomaly and mean vertical profiles of zonal wind and potential temperatures at Kototabang (upper panels) and Jambi (lower panels), averaged separately for days when westward (lefthand-side panels) or eastward (righthand-side panels) migrations of cloud systems were observed in November 2001. The profiles show potential temperature θ (thinner solid line), equivalent temperature θ_e (thinner dashed-dotted line), saturated equivalent temperature θ_e^* (thinner dotted line) and zonal wind (thicker solid line) averaged for days of cloud migrations of each direction, and monthly mean of zonal wind (thicker dotted line).

Figure 8. Same as Figure 3 but for a cross-section CC' every month during May 2001–April 2002.

Figure 9. Time-longitude cross-section of horizontal wind (arrows, upward is northward) and zonal wind (contours, every 3 ms^{-1} ; shade represents easterly) at 850 hPa level on the equator during May 2001–April 2002, based on the NCEP/NCAR objective analysis. The solid lines indicate the ends of Sumatera Island.

Figure 10. Latitude-time cross-sections (along 100°E during May 2001–April 2002) of (a) occurrence frequency α of cloud systems (cloud top temperature is between 170 and 270 K) (see Subsection 2.1.1), and (b) 300- and (c) 850-hPa horizontal wind (arrows: upward is northward; shaded represents easterly in (b) and westerly in (c)) based on the NCEP/NCAR objective analysis.

Figure 11. Schematic pictures of relationships between observed zonal wind anomalies in lower (1.5–5.5 km) and upper (10–12 km) altitudes at each local time and convergence/divergence associated with a cloud system migrating westward (left panels) or eastward (right panels).

Figure 12. Schematic picture of seasonal cycle of geographical distributions of ITCZ (shaded) and migrating cloud systems in around Sumatera Island.

Table 1: Migratory distance and speed of tall cloud systems (cloud top temperature ≤ 230 K) along each cross-section over Sumatera Island in November 2001.

	Westward migration		Eastward migration	
	distance	speed	distance	speed
	(km)	(ms ⁻¹)	(km)	(ms ⁻¹)
AA'	155	4.3	137	2.9
BB'	250	5.3	152	3.2
CC'	221	5.6	291	6.7
DD'	265	6.7	407	9.4
EE'	174	4.0	263	5.2

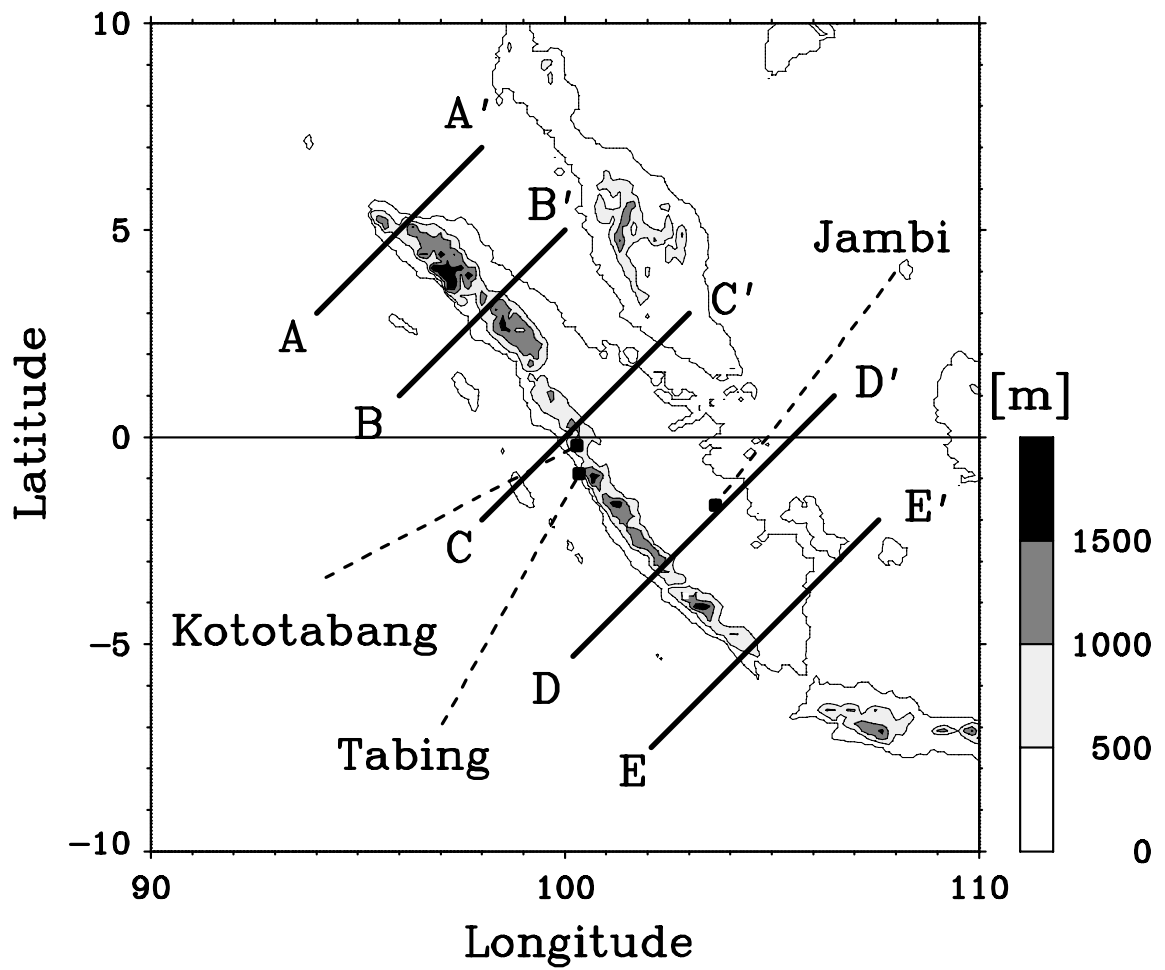


Figure 1: Topography of Sumatra Island. Tabing, Kototabang, and Jambi are stations operated for intensive observational periods in 2001 and 2002. Along five lines from AA' to EE', diurnal cycle of cloud system migration will be analyzed in subsequent figures and sections.

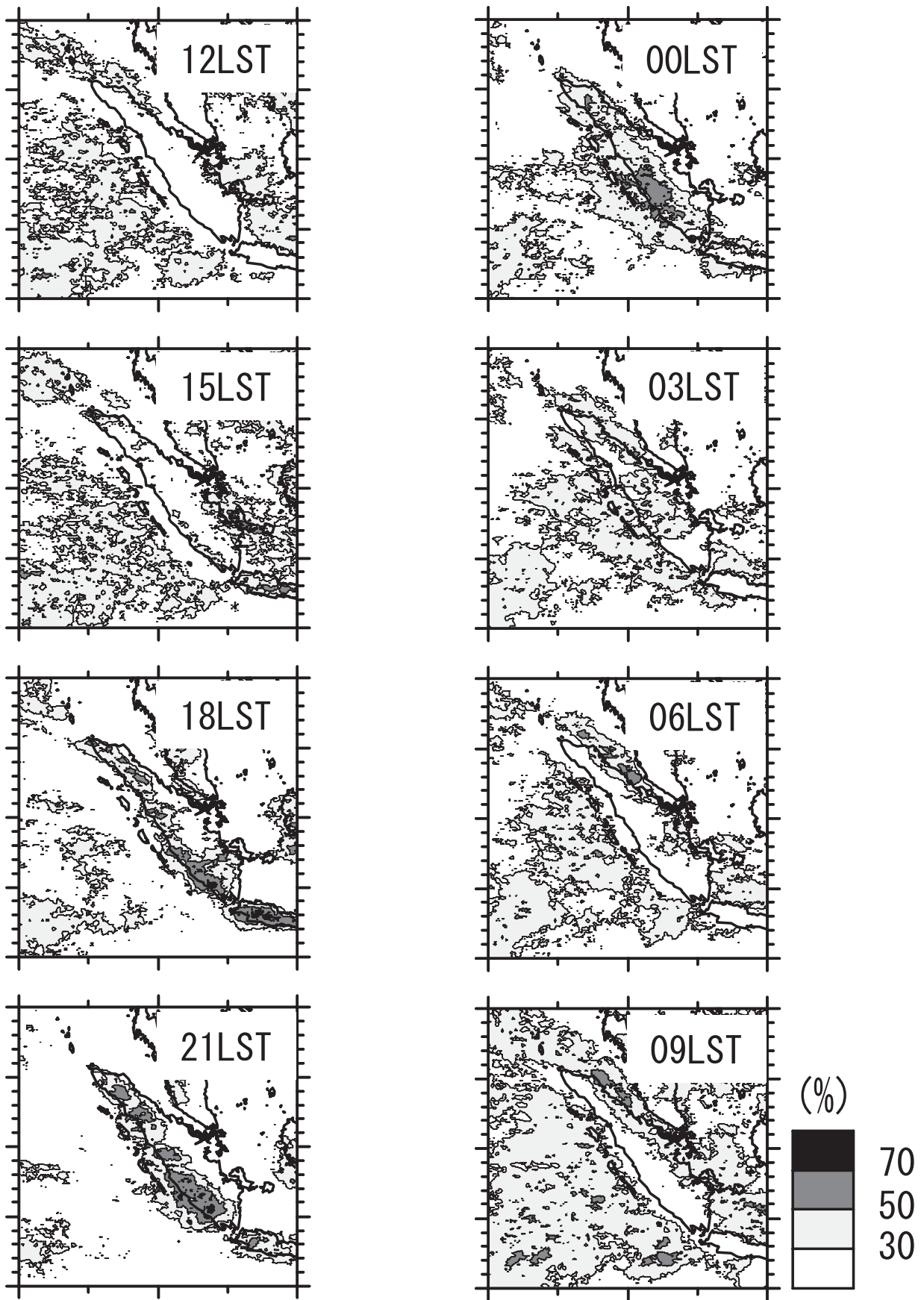


Figure 2: Horizontal distributions of the occurrence frequency α of tall cloud systems (cloud top temperature ≤ 230 K) at each pixel and time every 3 hour over Sumatra Island and surroundings in November 2001. Definition of α is given by (2) in the text.

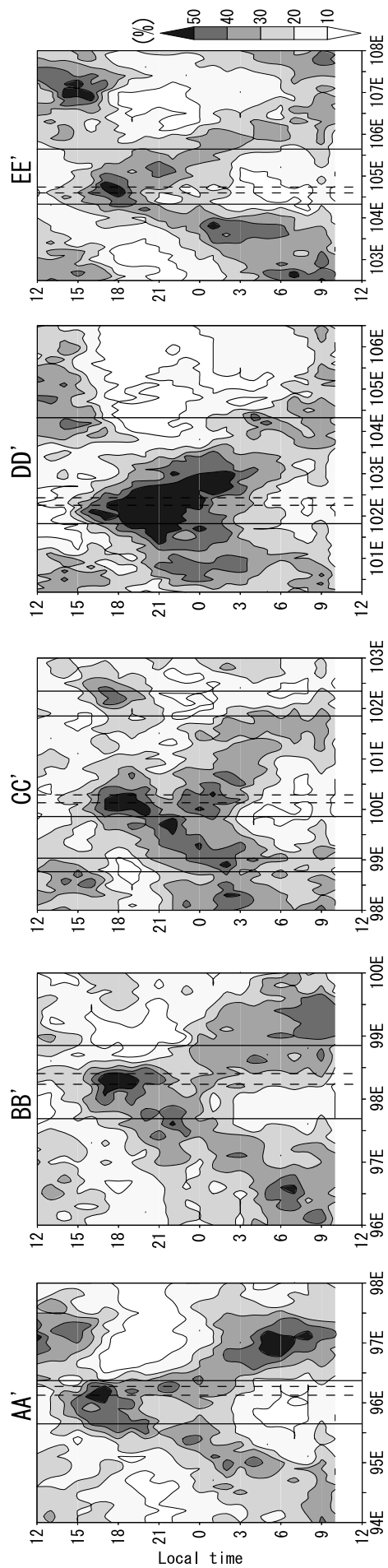


Figure 3: Local time-longitude cross-sections of the occurrence frequency α of tall cloud systems (cloud top temperature ≤ 230 K) at each pixel along the five lines from AA' to EE' shown in Figure 1 during November 2001. Vertical solid and broken lines represent locations of coasts of Sumatara Island (for CC') also of Mentawai Archipelago and Malay Peninsula) and of 800 m MSL, respectively.

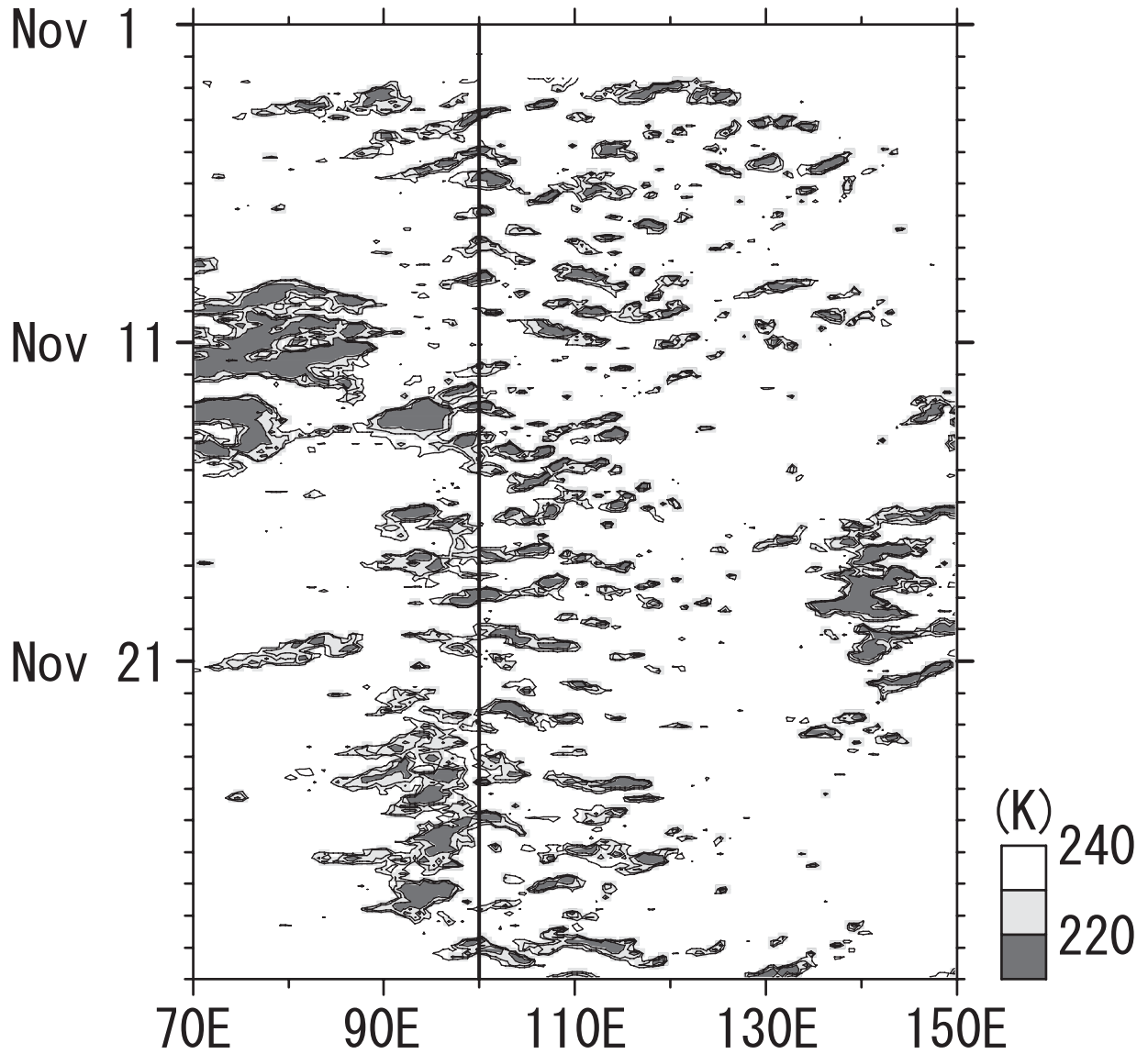


Figure 4: Time-longitude cross-section of T_{BB} on the equator in November 2001, based on GMS IR1 data with a spatial resolution of $0.5^\circ \times 0.5^\circ$ grid points. The vertical solid line indicates 100°E which corresponds to the location of the central mountain range of Sumatera Island on the equator.

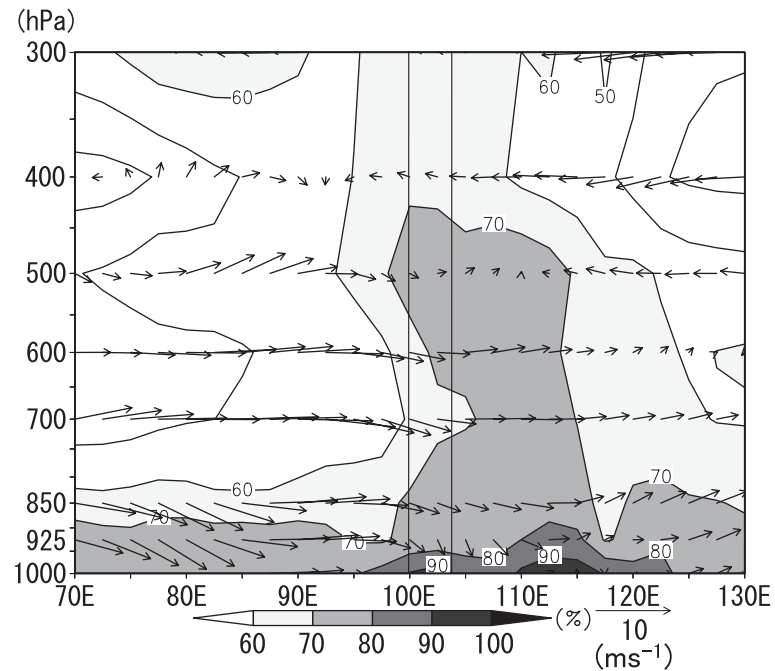


Figure 5: Vertical-zonal cross-section of horizontal wind (arrows; upward is northward) and relative humidity (shaded is larger than 60 %) on the equator at 12 UTC (19 LST) averaged for November 2001, based on the NCEP/NCAR objective analysis. The solid lines indicate the coasts of Sumatra Island.

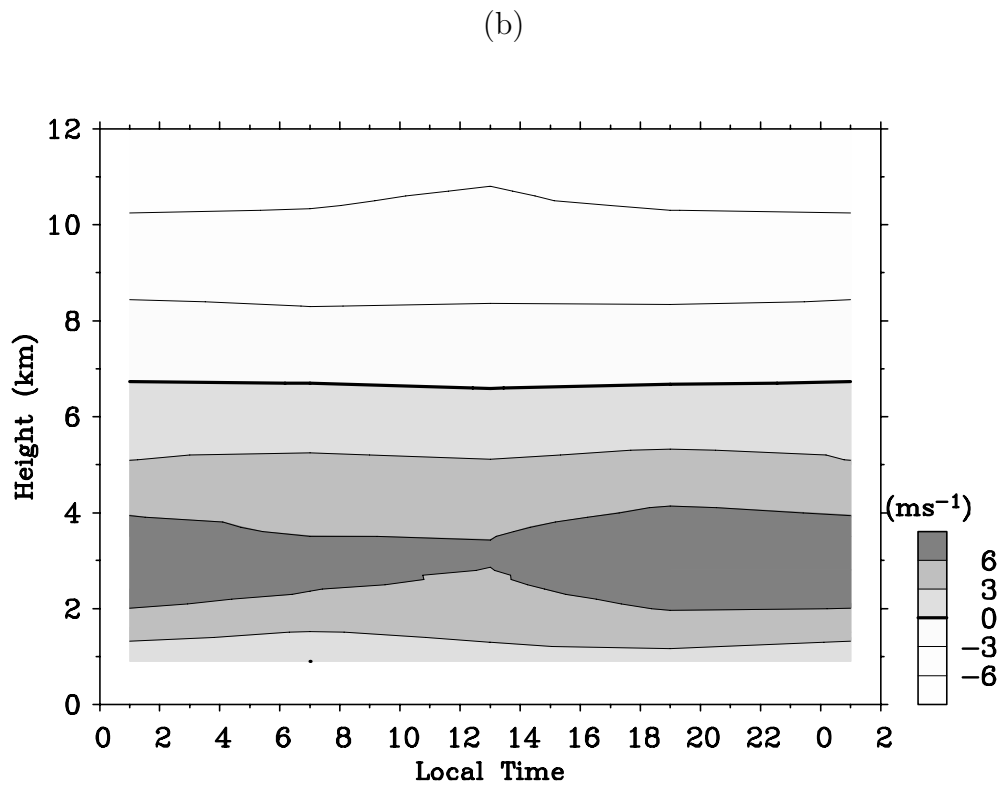
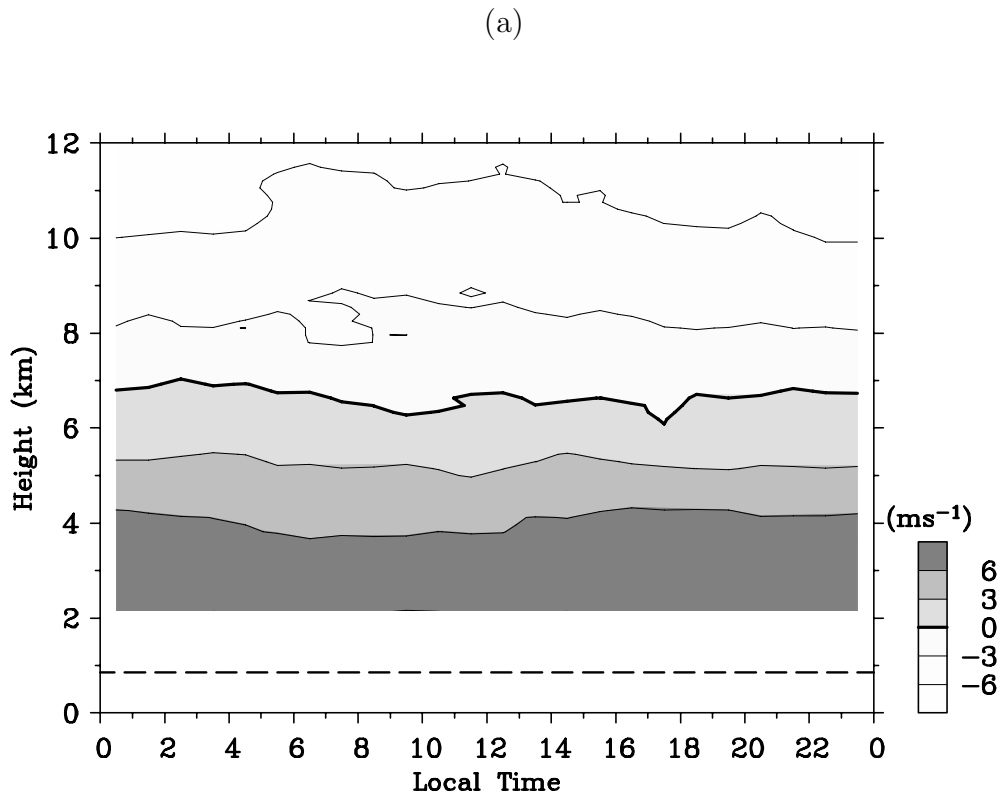


Figure 6: Vertical-local time cross-sections of mean diurnal variation of zonal wind observed with (a) EAR and (b) rawinsondes at Kototabang in November 2001. Broken line in (a) represents the altitude at Kototabang (865 m).

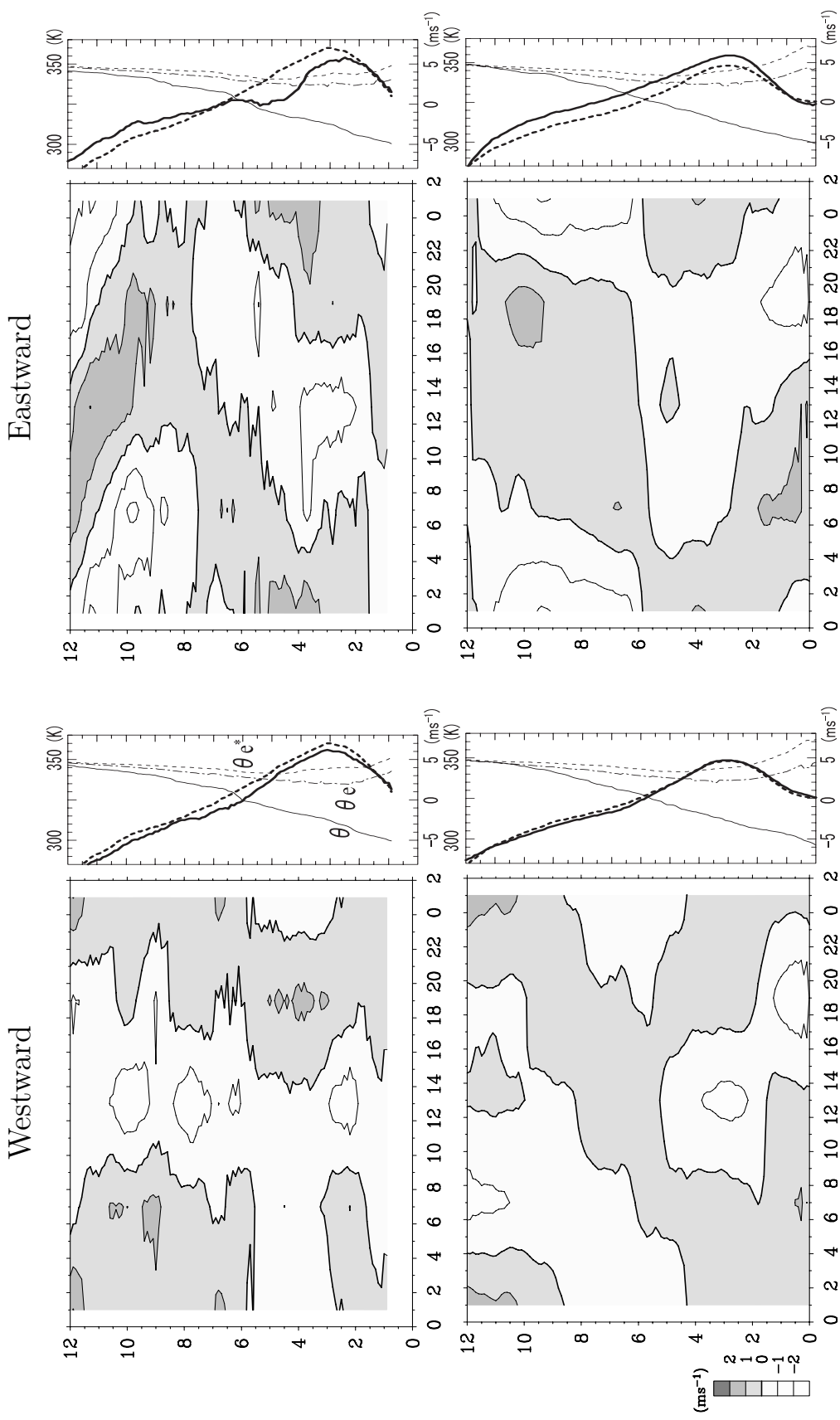


Figure 7: Vertical-local time cross-sections of zonal wind anomaly and mean vertical profiles of zonal wind and potential temperatures at Kototabang (upper panels) and Jambi (lower panels), averaged separately for days when westward (lefthand-side panels) or eastward (righthand-side panels) migrations of cloud systems were observed in November 2001. The profiles show potential temperature θ (thinner solid line), equivalent potential temperature θ_e^* (thinner dashed-dotted line), saturated equivalent potential temperature θ_e^* (thinner dotted line) and zonal wind (thicker solid line) averaged for days of cloud migrations of each direction, and monthly mean of zonal wind (thicker dotted line).

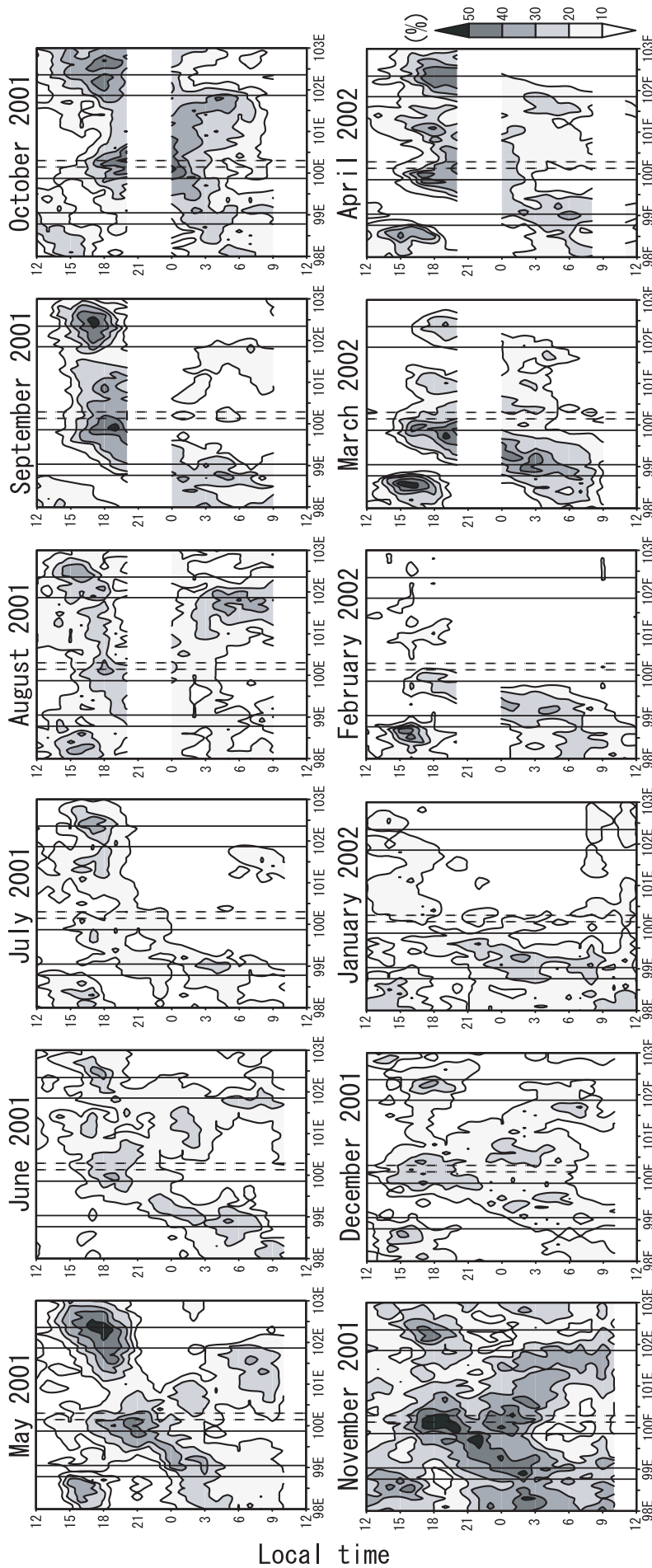


Figure 8: Same as Figure 3 but for a cross-section CC' every month during May 2001–April 2002.

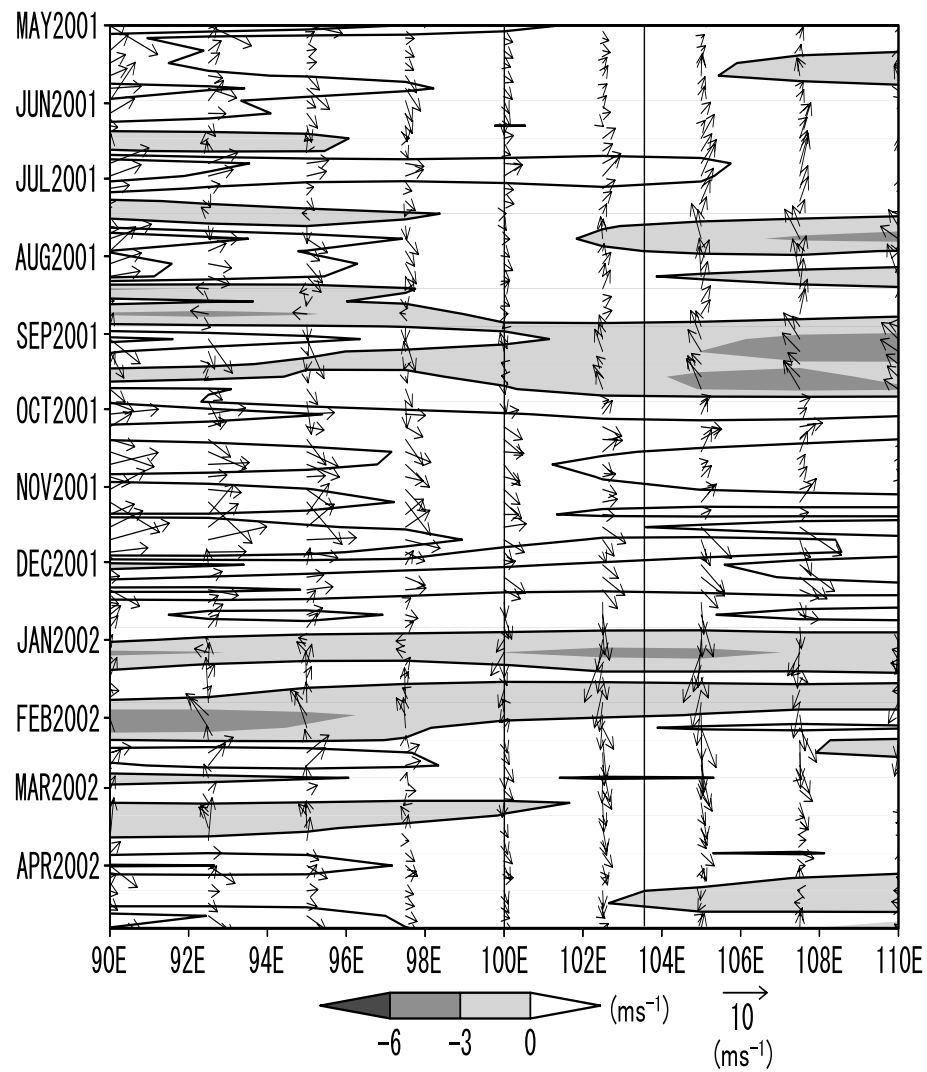


Figure 9: Time-longitude cross-section of horizontal wind (arrows, upward is northward) and zonal wind (contours, every 3 ms^{-1} ; shade represents easterly) at 850 hPa level on the equator during May 2001–April 2002, based on the NCEP/NCAR objective analysis. The solid lines indicate the ends of Sumatra Island.

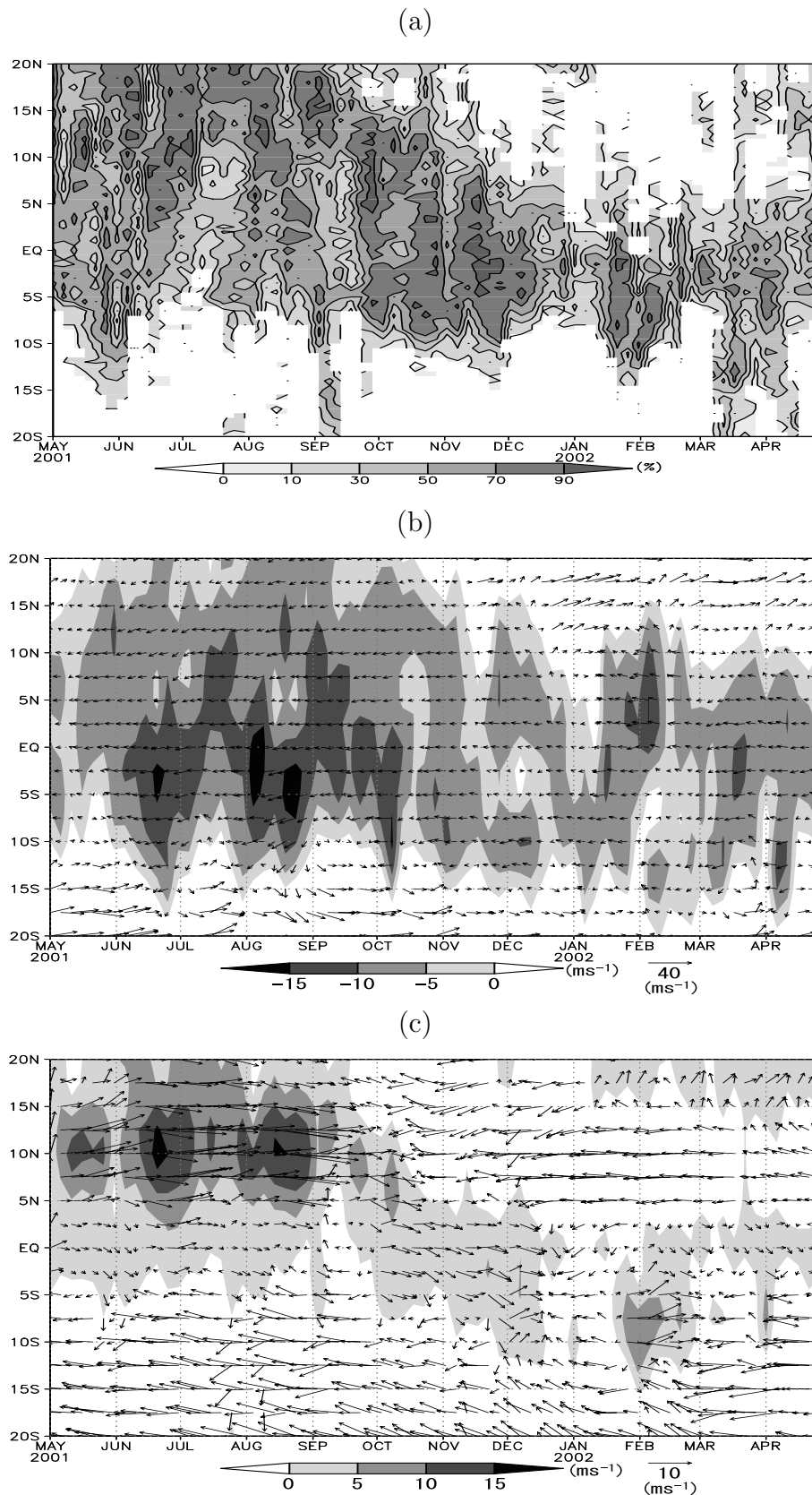


Figure 10: Latitude-time cross-sections (along 100°E during May 2001–April 2002) of (a) occurrence frequency α of cloud systems (cloud top temperature is between 170 and 270 K) (see Subsection 2.1.1), and (b) 300- and (c) 850-hPa horizontal wind (arrows: upward is northward; shaded represents easterly in (b) and westerly in (c)) based on the NCEP/NCAR objective analysis.

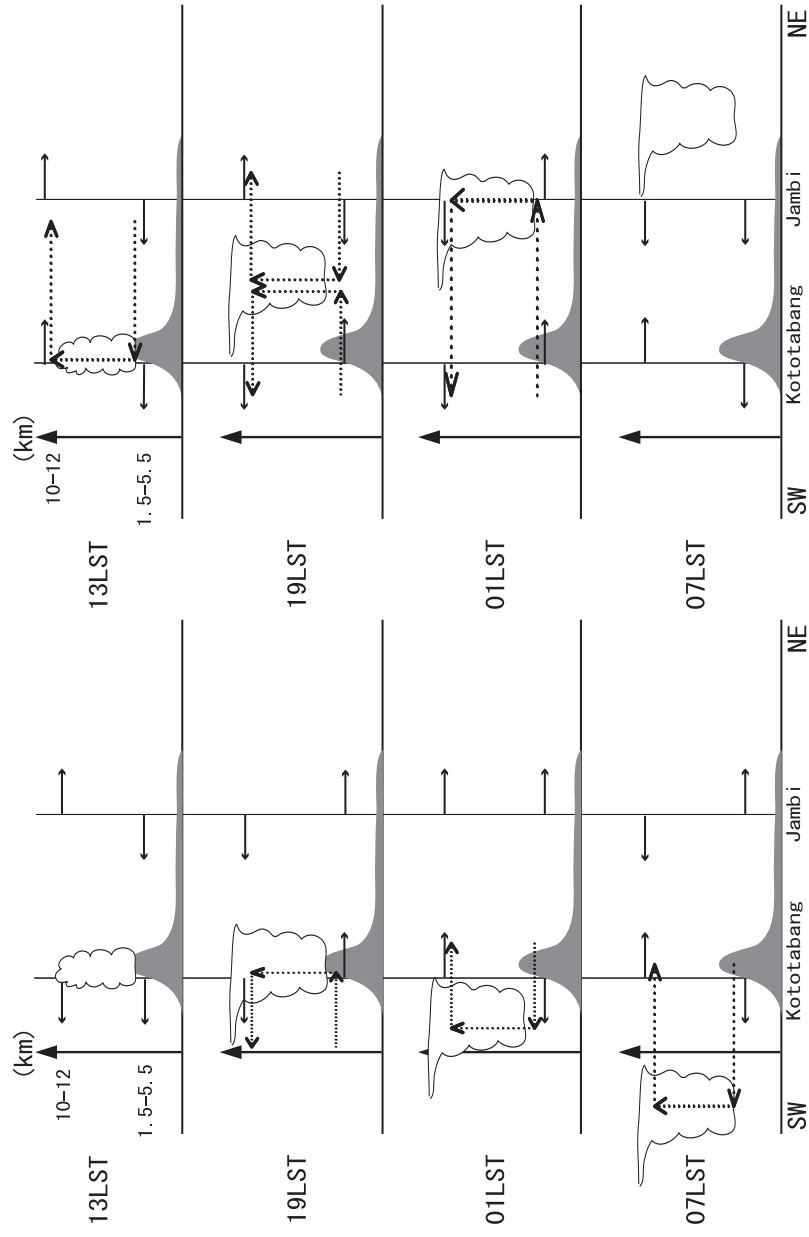


Figure 11: Schematic pictures of relationships between observed zonal wind anomalies in lower (1.5–5.5 km) and upper (10–12 km) altitudes at each local time and convergence/divergence associated with a cloud system migrating westward (left panels) or eastward (right panels).

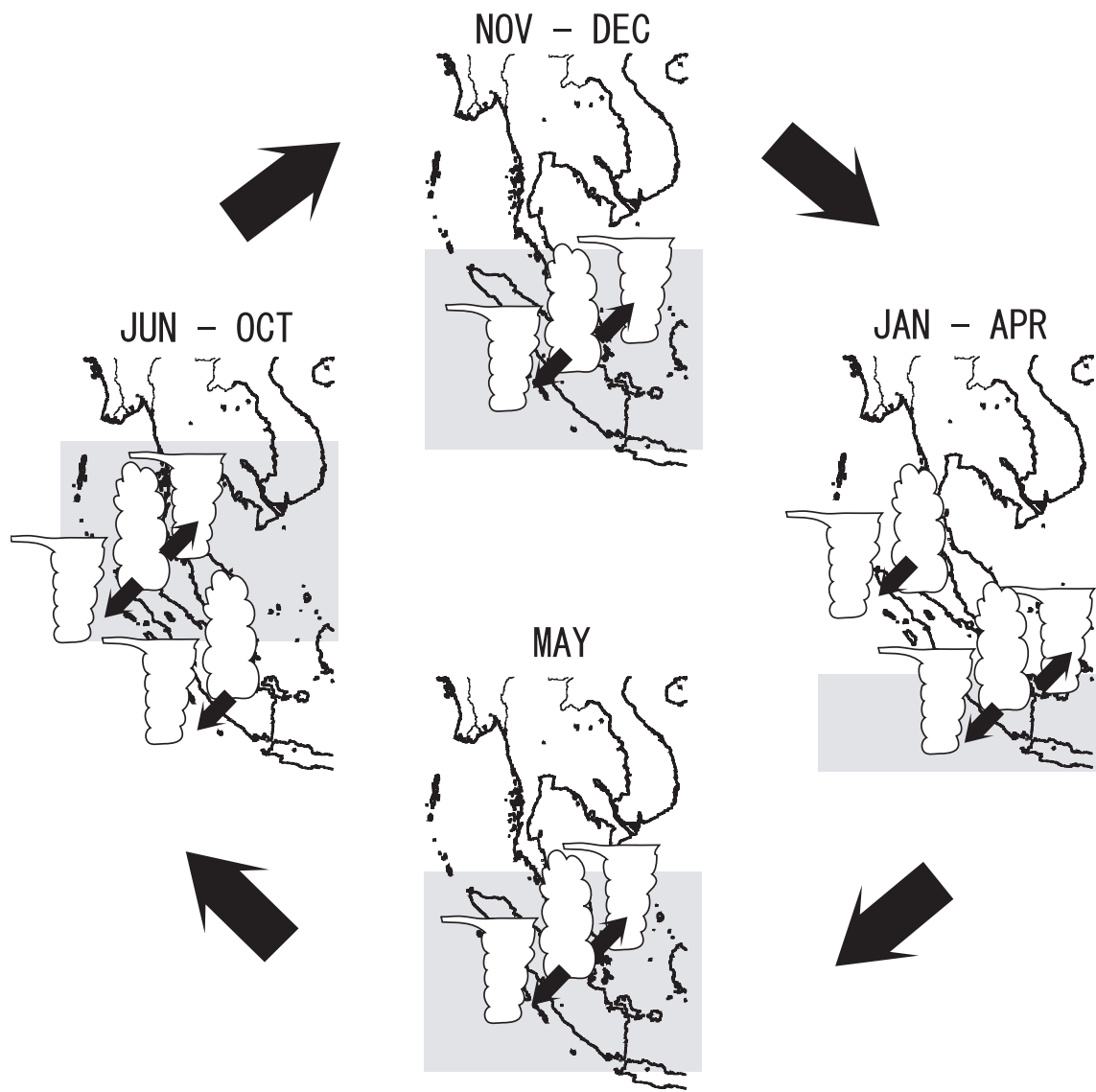


Figure 12: Schematic picture of seasonal cycle of geographical distributions of ITCZ (shaded) and migrating cloud systems in around Sumatra Island.